

## Mössbauer study of the Fe-doped $\text{La}_{0.9}\text{MnO}_x$ manganites

This article has been downloaded from IOPscience. Please scroll down to see the full text article.

2004 J. Phys.: Condens. Matter 16 4335

(<http://iopscience.iop.org/0953-8984/16/24/015>)

View [the table of contents for this issue](#), or go to the [journal homepage](#) for more

Download details:

IP Address: 129.252.86.83

The article was downloaded on 27/05/2010 at 15:34

Please note that [terms and conditions apply](#).

# Mössbauer study of the Fe-doped $\text{La}_{0.9}\text{MnO}_x$ manganites

M Kopcewicz<sup>1</sup>, V A Khomchenko<sup>2,4</sup>, I O Troyanchuk<sup>2</sup> and H Szymczak<sup>3</sup>

<sup>1</sup> Institute of Electronic Materials Technology, Wolczynska street 133, 01-919 Warsaw, Poland

<sup>2</sup> Institute of Solid State and Semiconductor Physics, NAS, P. Brovka street 17, 220072 Minsk, Belarus

<sup>3</sup> Institute of Physics, PAS, Lotnikow street 32/46, 02-668 Warsaw, Poland

E-mail: khomchen@ifftp.bas-net.by

Received 1 April 2004

Published 4 June 2004

Online at [stacks.iop.org/JPhysCM/16/4335](http://stacks.iop.org/JPhysCM/16/4335)

doi:10.1088/0953-8984/16/24/015

## Abstract

The local structure of the 2.5%  $^{57}\text{Fe}$ -doped  $\text{La}_{0.9}\text{MnO}_x$  ( $x = 2.89, 2.92$  and  $2.93$ ) manganites has been investigated by means of Mössbauer spectroscopy. In the paramagnetic phase, the Mössbauer spectra of all three samples consist of two quadrupole doublets which suggest two different iron positions distinguished by their local environment. It has been assumed that in the position with a large quadrupole splitting, QS1, the  $\text{Fe}^{3+}$  is surrounded by six Jahn–Teller  $\text{Mn}^{3+}$  ions. The second iron position with the smaller quadrupole splitting, QS2, corresponds to the manganese environment in which at least one manganese ion is in the  $\text{Mn}^{4+}$  state. In the magnetically ordered phase, these positions become indistinguishable. We conclude that even in the absence of  $\text{Mn}^{4+}$  ions the introduction of the non-Jahn–Teller  $\text{Fe}^{3+}$  ion in the  $\text{Mn}^{3+}$  environment leads to the local removal of static ordering of the  $\text{Mn}^{3+}$   $d_{3z^2-r^2}$  orbitals that result in the ferromagnetic ordering of the Mn spins. The result indicates a key role of the dynamic orbital correlations in the formation of the ferromagnetic ordering in manganites.

## 1. Introduction

Hole-doped lanthanum manganites with a perovskite structure have attracted great attention due to the close relationship between their structural, magnetic and transport properties. The parent compound  $\text{La}^{3+}\text{Mn}^{3+}\text{O}_3^{2-}$  is an A-type antiferromagnetic insulator with  $T_N = 140$  K [1]. A heterovalent cation substitution or creation of cation vacancies gives rise to the appearance of  $\text{Mn}^{4+}$  ions. As a result, at a certain doping range (about 10% of  $\text{Mn}^{4+}$  ions) the ground

<sup>4</sup> Author to whom any correspondence should be addressed.

state of the manganites becomes an insulating ferromagnet (FMI). With further increase of the hole concentration (about 17–20% of  $\text{Mn}^{4+}$ ), the transition to the ferromagnetic metallic state (FMM) is observed [2, 3]. Initially, the existence of the ferromagnetic metallic phase in manganites was attributed to the double exchange interaction [4]. In the double exchange model, strong Hund's rule coupling enhances the hopping of  $e_g$  electrons in the successive  $\text{Mn}^{3+}$  and  $\text{Mn}^{4+}$  ions by establishing ferromagnetic spin ordering. More recently, theoretical [5, 6] and experimental [7–9] investigations have shown that double exchange is inadequate for the explanation of the complex magnetic phase diagram of manganites and that the Jahn–Teller (JT) effect plays an essential role.

Recent research on La-deficient colossal magnetoresistive  $\text{La}_{0.88}\text{MnO}_x$  ( $2.82 \leq x \leq 2.96$ ) manganites, performed with x-ray, neutron diffraction, Young's modulus, magnetization and resistivity measurements, has revealed a strong correlation between the magnetic and orbital states of the samples under study [10]. The compounds with a strong antiferromagnetic component have been found to exhibit a cooperative orbital ordering, while ferromagnetic samples are orbitally disordered. Immediate information about a coupling of spin with orbital and lattice degrees of freedom may be obtained with Mössbauer spectroscopy. A few per cent of  $^{57}\text{Fe}$  substitution for Mn in manganites is sufficient as a micro-probe detecting the local structure and magnetic state of the Fe environment in Mössbauer experiments because quadrupole splitting is very sensitive to the distribution of the electrons which surround the resonant nuclei, and magnetic hyperfine splitting depends on the magnetic ordering of the surrounding ions. In this paper we present the results of the Mössbauer measurements performed for samples of the  $\text{La}_{0.9}\text{MnO}_x$  manganites doped with 2.5% of  $^{57}\text{Fe}$ . We confirm that magnetic properties of the manganites are determined by the type of their orbital state and that the ferromagnetic ordering arises from dynamic correlations of the  $d_{3z^2-r^2}$  orbitals of the  $\text{Mn}^{3+}$  ions.

## 2. Experiment

The polycrystalline sample  $\text{La}_{0.9}\text{Mn}_{0.975}\text{Fe}_{0.025}\text{O}_x$  was prepared by a solid-state reaction method using high-purity  $\text{La}_2\text{O}_3$ ,  $\text{MnO}_2$  and  $\text{Fe}_2\text{O}_3$  reagents. To remove absorbed water, a pre-firing of  $\text{La}_2\text{O}_3$  (1000 °C, 2 h) was carried out. After that, the compacted mixture of reagents taken in stoichiometric cation ratio was annealed at 1350, 1150 and 1050 °C in air for 24 h and then slowly cooled at a rate of 30 °C  $\text{h}^{-1}$ . The oxygen content of the resulting material was determined using thermogravimetric analysis (TGA) by decomposition of the sample into  $\text{La}_2\text{O}_3$ ,  $\text{MnO}$  and  $\text{Fe}$  in a reducing  $\text{H}_2/\text{N}_2$  flow. The estimation of the oxygen content led to the nominal chemical formula  $\text{La}_{0.9}\text{Mn}_{0.975}\text{Fe}_{0.025}\text{O}_{2.93}$  with an error of  $\pm 0.01$  oxygen per formula. Reduction of the samples was carried out in evacuated quartz ampoules at  $T = 1050$  °C for 24 h. Metallic tantalum was used as reducing agent. According to the TGA data, the oxygen indexes in the reduced compounds were  $x = 2.92 \pm 0.01$  and  $2.89 \pm 0.01$ .

The unit cell parameters as well as the phase purity of the samples were checked by x-ray diffraction analysis using a DRON-3M diffractometer with  $\text{Cu K}\alpha$  radiation. The data were analysed with the FULLPROF program [11]. The magnetization measurements were made with a commercial vibrating sample magnetometer OI-3001. The Mössbauer measurements were performed using a conventional constant acceleration spectrometer with a  $^{57}\text{Co}$ -in-Rh source. The spectra were recorded in transmission geometry at temperatures ranging from 80 to 300 K. A continuous flow Oxford Instruments CF-100 cryostat was used. The Mössbauer spectra were fitted using the NORMOS program [12], assuming the superposition of the hyperfine field distribution  $P(H)$  component and two discrete quadrupole splitting ones.

**Table 1.** Unit cell parameters of the  $\text{La}_{0.9}\text{Mn}_{0.975}\text{Fe}_{0.025}\text{O}_x$  manganites at room temperature.

Sample	Space group	$a$ (Å)	$b$ (Å)	$c$ (Å)	$\alpha$ (deg)	$\beta$ (deg)	$\gamma$ (deg)	$V$ (Å <sup>3</sup> )
$x = 2.89$	<i>Pnma</i>	5.5874	7.7311	5.5232	90	90	90	238.58
$x = 2.92$	<i>Pnma</i>	5.5213	7.7801	5.5271	90	90	90	237.42
$x = 2.93$	<i>I2/a</i>	7.7804	5.5327	5.4721	90	90.66	90	235.54

### 3. Results

The x-ray diffraction analysis showed that all the synthesized samples were single phase. The  $x = 2.89$  and  $2.92$  samples present a *Pnma* orthorhombic space group (table 1). The former is characterized by  $O'$ -orthorhombic type unit cell distortion ( $b/\sqrt{2} < c < a$ ), the latter exhibits O-orthorhombic symmetry ( $b/\sqrt{2} \approx c \approx a$ ). The unit cell of the most oxidized  $\text{La}_{0.9}\text{Mn}_{0.975}\text{Fe}_{0.025}\text{O}_{2.93}$  compound has monoclinic distortions (space group *I2/a*). The unit cell volume of the samples gradually decreases as the oxygen concentration increases. Such a decrease is consistent with the expectation from the difference in ionic radii of  $\text{Mn}^{3+}$  and  $\text{Mn}^{4+}$  ions [13].

The temperature dependences of magnetization for samples of  $\text{La}_{0.9}\text{Mn}_{0.975}\text{Fe}_{0.025}\text{O}_x$ , with  $x = 2.89, 2.92$  and  $2.93$  are shown in figure 1. The magnetic ordering temperatures, defined as the inflection points of the  $M$  versus  $T$  curves, are 117, 170 and 179 K, respectively. For all the samples, ZFC magnetization shows a maximum at 110 K. In the case of the  $x = 2.92$  and  $2.93$  samples, this maximum is accompanied by a break in the FC curve. Significant thermomagnetic irreversibility indicating the large magnetic anisotropy of the samples [14] begins to develop below this temperature. The value of magnetization estimated for the  $x = 2.89$  compound in a field of 15 kOe suggests the presence of a significant ferromagnetic contribution (figure 2). The increase of magnetization and decrease of coercive field are observed with increasing oxygen content (figure 2).

Mössbauer spectra obtained for these samples at different temperatures are shown in figures 3–5. The hyperfine parameters resulting from the fitting are summarized in table 2. As suggested from the fitting, the room temperature Mössbauer spectra of the samples consist of two well defined quadrupole doublets that signify two different iron positions in the  $\text{La}_{0.9}\text{Mn}_{0.975}\text{Fe}_{0.025}\text{O}_x$  lattice. Some Fe ions are located at low symmetry lattice positions, as evidenced by the large value of quadrupole splitting QS1, whereas for other Fe ions the local symmetry is higher (QS2 < QS1). Both QS1 and QS2 quadrupole splittings decrease with increasing oxygen content and increase with decreasing temperature. Both doublets have similar room temperature isomer shift values that are typical of high-spin  $\text{Fe}^{3+}$  in octahedral coordination [15]. The relative spectral area of the quadrupole doublets allows the determination of the relative fractions of Fe ions in the corresponding lattice positions. In the case of the  $x = 2.89$  sample, about 45% of Fe ions are located at the site with large quadrupole splitting QS1  $\approx 0.69 \text{ mm s}^{-1}$ . About 55% of Fe ions occupy positions with smaller QS2  $\approx 0.38 \text{ mm s}^{-1}$  (figure 6(a)). An increase of the relative fraction of Fe ions at the high symmetry lattice position, with quadrupole splitting QS2, is observed for  $x = 2.92$  and  $2.93$  compounds (figures 6(b), (c)). For all samples, the relative spectral areas of the quadrupole doublets in the paramagnetic phase are temperature independent within statistical error (figure 6).

The Mössbauer spectrum obtained for the sample with  $x = 2.89$  at 120 K indicates the appearance of magnetic ordering (figure 3(d)). The relative spectral area of the magnetic component increases strongly with decreasing temperature at the expense of the paramagnetic

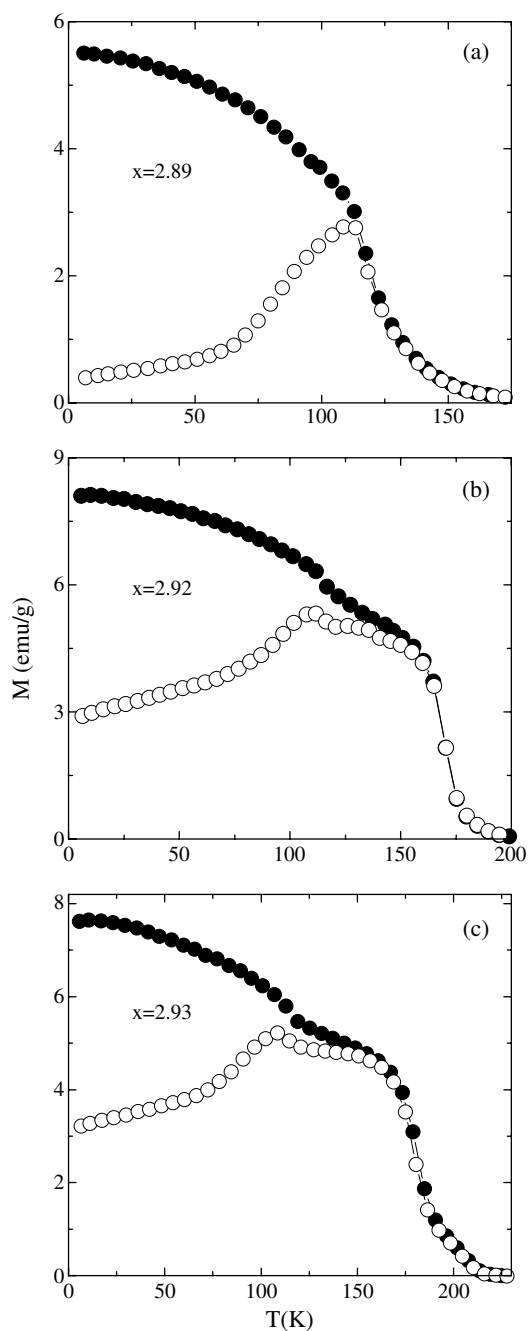


**Figure 1.** Temperature dependences of the magnetization of the  $\text{La}_{0.9}\text{Mn}_{0.975}\text{Fe}_{0.025}\text{O}_x$  samples, measured in a field of 100 Oe. Open and closed symbols correspond to data obtained in zero-field-cooled (ZFC) and field-cooled (FC) modes, respectively.

fraction (figure 6(a)). At the temperature of 110 K, the spectral contribution from the quadrupole doublets disappears, and the spectrum is fitted with one Zeeman component

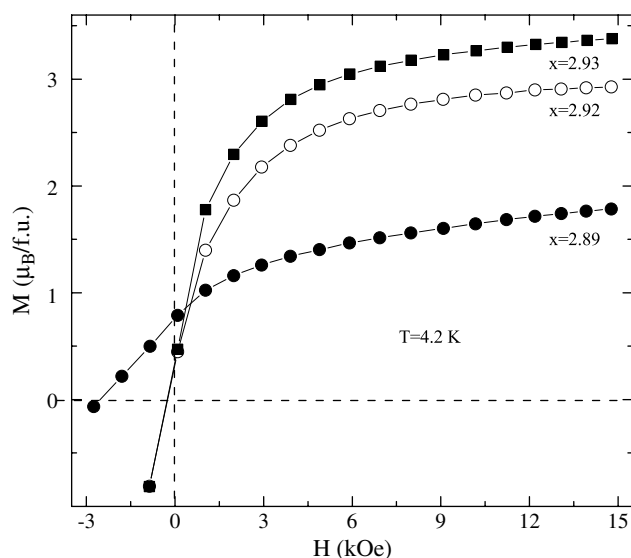


**Figure 2.** Field dependences of the magnetization for the  $\text{La}_{0.9}\text{Mn}_{0.975}\text{Fe}_{0.025}\text{O}_x$  compounds at a temperature of 4.2 K.

resulting from the distribution of hyperfine field  $P(H)$  (figure 3(e)). Thus, two different Fe positions observed for the paramagnetic state become indistinguishable in the magnetic phase. The shape of the Mössbauer spectra obtained below 110 K suggests a wide distribution of hyperfine fields. The hyperfine field  $H$  corresponding to the main peak in the relevant hyperfine field distribution  $P(H)$  reaches the value of 40.5 T at 80 K, confirming that iron is in the  $\text{Fe}^{3+}$  high-spin state ( $S = 5/2$ ).

For the  $x = 2.92$  sample, the transition from the paramagnetic to the magnetically ordered state occurs in the broader temperature range (figure 6(b)). The magnetic ordering already appears at 160 K (figure 4(c)). The quadrupole QS1 and QS2 components coexist with the magnetically ordered phase down to about 110 K (figure 4(f)). As in the case of the  $\text{La}_{0.9}\text{Mn}_{0.975}\text{Fe}_{0.025}\text{O}_{2.98}$  solid solution, the magnetic phase is fitted with the hyperfine field distribution  $P(H)$ . The hyperfine field value, corresponding to the main peak in the  $P(H)$  distribution, is 46.5 T at 80 K (table 2). The similar temperature evolution of the Mössbauer spectra is observed for the  $x = 2.93$  sample (figures 5 and 6). The magnetic ordering temperatures defined with the Mössbauer experiments (figure 6) are in a good agreement with those obtained from the magnetization measurements (figure 1).

The main results are summarized as follows.

- (i) Iron in the  $\text{La}_{0.9}\text{Mn}_{0.975}\text{Fe}_{0.025}\text{O}_x$  lattice is in the  $\text{Fe}^{3+}$  state with a high spin electronic configuration  $t_{2g}^3 e_g^2$ .
- (ii) At higher temperatures (in the paramagnetic phase) the Mössbauer spectra of all three samples are fitted with two quadrupole doublets which may suggest two different iron positions distinguished by their local environment.
- (iii) At lower temperatures (in the magnetically ordered phase) these positions become indistinguishable.
- (iv) The quadrupole splittings QS1 and QS2 decrease with increasing oxygen content and increase with decreasing temperature.

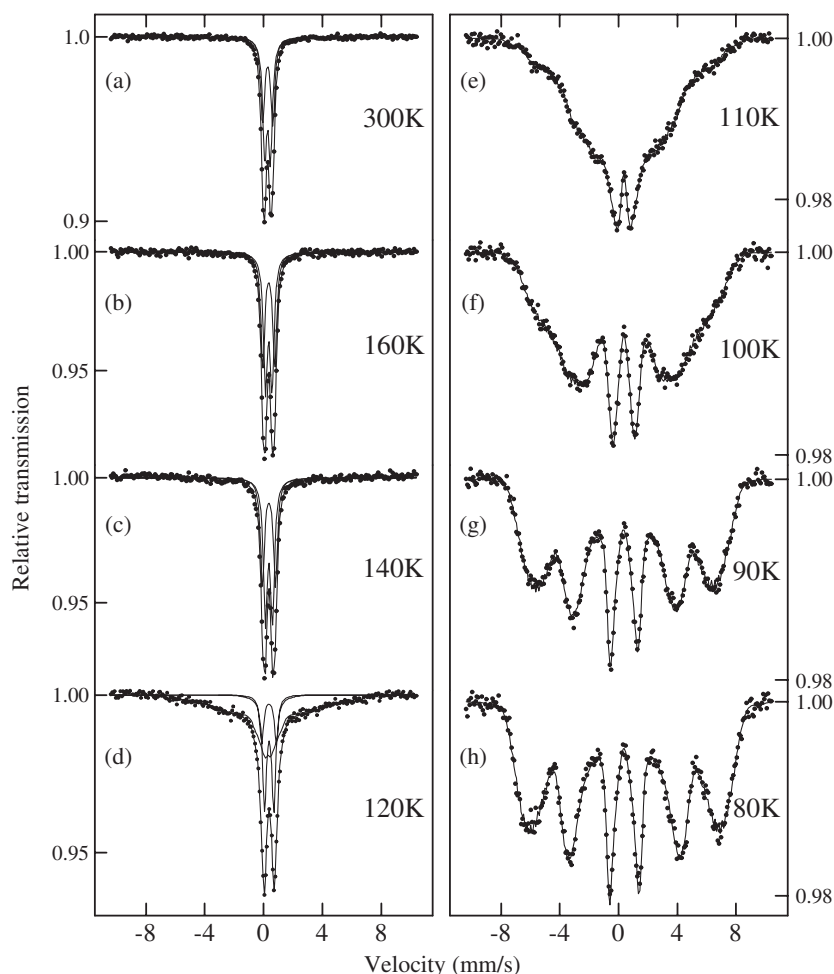


**Figure 3.** Mössbauer spectra for the  $x = 2.89$  sample at different temperatures.

- (v) The formation of magnetic ordering does not cause the simultaneous disappearance of the paramagnetic phase, which coexists with the magnetic state in a fairly wide temperature range. This temperature range increases with increasing  $\text{Mn}^{4+}$  concentration. The disappearance of the paramagnetic phase is accompanied by a cusp on the ZFC curve.

#### 4. Discussion

Let us recall that  $\text{Mn}^{3+}$  3d states in  $\text{LaMnO}_3$  are split by the cubic crystal field to the threefold degenerate  $t_{2g}$  and twofold degenerate  $e_g$  levels. The former lies lower than the latter; therefore four d electrons of the  $\text{Mn}^{3+}$  ion occupy the  $t_{2g}$  level completely and the  $e_g$  level only partly. This is the reason for the cooperative Jahn–Teller effect: it reduces the energy of such a degenerate system by lowering its symmetry which lifts the degeneracy of the  $e_g$  levels so that the electron can occupy the lowest of them. Analysis of the Mn–O bond lengths within the tetragonally distorted  $\text{MnO}_6$  octahedron in  $\text{LaMnO}_3$  indicates that the lower of the two  $e_g$  levels is the  $d_{3z^2-r^2}$  ( $z$  axis is local) sublevel [16]. The cooperative antiferrodistortive ordering

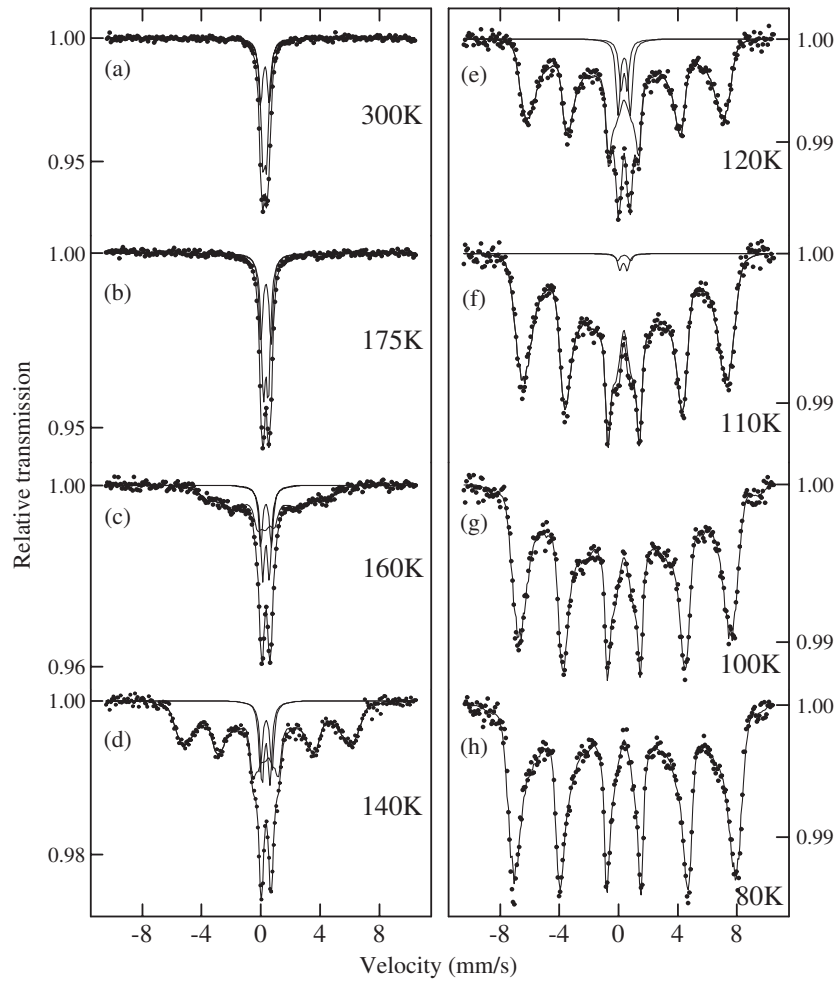


**Figure 4.** Mössbauer spectra for the  $x = 2.92$  sample at different temperatures.

of the  $d_{3z^2-r^2}$  orbitals manifests itself in the  $O'$ -orthorhombic symmetry of the crystal. The A-type antiferromagnetic structure peculiar to  $\text{LaMnO}_3$  is explained as arising from this orbital ordering [17].

Neutron diffraction studies have shown that  $\text{LaMnO}_3$  undergoes a structural transition from  $O'$ -orthorhombic to O-orthorhombic phase at  $T_{JT} = 750$  K [18]. The  $\text{MnO}_6$  octahedron in the O-orthorhombic phase becomes nearly regular, i.e. the orbital ordering disappears [18]. However, x-ray absorption near the edge structure and the extended x-ray absorption fine structure at the Mn K-edge measurements have revealed that the  $\text{MnO}_6$  octahedrons in  $\text{LaMnO}_3$  remain tetragonally distorted at  $T > T_{JT}$  [19]. The empty  $\text{Mn}^{3+}$  electronic d states were shown to be unaltered through the Jahn–Teller transition. The lowest energy for the  $e_g$  electron corresponds to the three possible distortions giving rise to three degenerate vibronic states,  $d_{x^2-r^2}$ ,  $d_{y^2-r^2}$  and  $d_{z^2-r^2}$  being the electronic orbitals of the vibronic state. The thermally excited electron jumps between these states above  $T_{JT}$  and is localized in an ordered state below  $T_{JT}$ . The orbital ordering proposed for  $\text{LaMnO}_3$  arises then from the ordering of the local Jahn–Teller distortions. The high temperature (O-orthorhombic) phase can be described



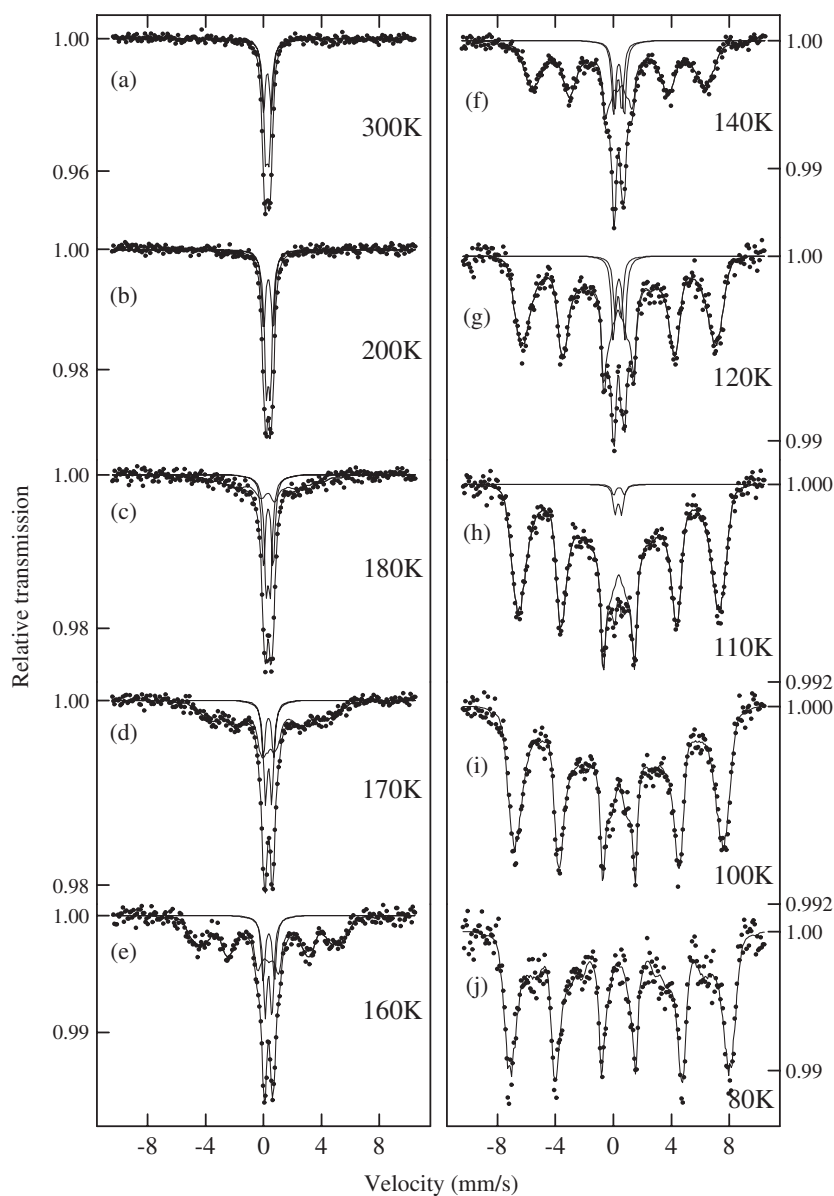


**Figure 5.** Mössbauer spectra for the  $x = 2.93$  sample at different temperatures.

as a dynamical locally distorted phase with the strong antiferrodistortive first neighbour coupling [19].

The similar situation seems to be observed for  $\text{Mn}^{4+}$ -doped manganites. The atomic pair-density function of  $\text{La}_{1-x}\text{Sr}_x\text{MnO}_3$  manganites ( $0 \leq x \leq 0.4$ ), obtained by pulsed neutron diffraction, indicates the existence of tetragonally distorted  $\text{MnO}_6$  octahedrons even in the rhombohedral metallic phase, when the crystallographic structure shows no JT distortions [20]. This is possible only in the case of the dynamic orbital correlations described above. One can assume that when one puts non-Jahn–Teller  $\text{Mn}^{4+}$  ions in the background of the  $\text{Mn}^{3+}$  ions,

**Table 2.** Experimental values of the isomer shift  $\delta$  relative to the  $\alpha$ -Fe standard, the quadrupole splitting QS, and the hyperfine magnetic field  $H$  for  $x = 2.89, 2.92$  and  $2.93$  samples at different temperatures.

Sample	$T$ (K)	$\delta 1$ ( $\text{mm s}^{-1}$ )	$\delta 2$ ( $\text{mm s}^{-1}$ )	QS1 ( $\text{mm s}^{-1}$ )	QS2 ( $\text{mm s}^{-1}$ )	$H$ (T)
$x = 2.89$	300	0.39	0.38	0.69	0.38	0
	160	0.46	0.46	0.81	0.45	0
	140	0.48	0.48	0.88	0.48	0
	120	0.48	0.49	0.99	0.63	16
	110	—	—	—	—	16
	100	—	—	—	—	27
	90	—	—	—	—	37.5
	80	—	—	—	—	40.5
$x = 2.92$	300	0.39	0.38	0.60	0.26	0
	190	0.45	0.45	0.67	0.32	0
	175	0.46	0.45	0.69	0.33	0
	160	0.46	0.46	0.73	0.45	24
	140	0.48	0.47	0.78	0.52	35
	120	0.49	0.48	0.84	0.43	41.5
	110	0.49	0.45	0.88	0.49	43
	100	—	—	—	—	44.5
80	—	—	—	—	46.5	
$x = 2.93$	300	0.38	0.37	0.55	0.25	0
	200	0.44	0.44	0.66	0.29	0
	180	0.44	0.44	0.66	0.29	16
	170	0.46	0.46	0.72	0.43	25
	160	0.47	0.45	0.78	0.47	30
	140	0.49	0.45	0.74	0.50	37
	120	0.49	0.44	0.79	0.43	42
	110	0.50	0.45	0.74	0.44	43.4
100	—	—	—	—	44.8	
80	—	—	—	—	47.0	

the  $e_g$  orbitals of all the  $\text{Mn}^{3+}$  ions surrounding the localized hole ( $\text{Mn}^{4+}$ ) tend to be directed towards it, forming an orbital polaron [21]. Due to the strong antiferrodistortive  $\text{Mn}^{3+}$  first neighbour coupling [19], dynamic correlations of the  $d_{3z^2-r^2}$  orbitals should arise.

According to the rules for  $180^\circ$  superexchange the dynamic orbital correlations lead to ferromagnetic interaction between the  $\text{Mn}^{3+}$  ions [22]. Hence, one can expect that ferromagnetism in manganites can arise even in the absence of  $\text{Mn}^{4+}$  ions, if only the JT effect is dynamic. Indeed, Mn substitution with non-Jahn–Teller diamagnetic  $\text{Nb}^{5+}$ ,  $\text{Al}^{3+}$ ,  $\text{Sc}^{3+}$ , etc, ions results in the appearance of ferromagnetic order [23, 24]. It is worth noting that the possibility of the existence of ferromagnetic ordering in the manganites, despite the absence of  $\text{Mn}^{4+}$  ions, rejects the double exchange concept. High-spin  $\text{Fe}^{3+}$  is a non-Jahn–Teller ion, therefore one can expect the appearance of the dynamic orbital correlations in the  $\text{Mn}^{3+}$  environment, which should lead to ferromagnetic ordering.

Owing to the lifetime of the excited nuclear state, the  $^{57}\text{Fe}$  nucleus is sensitive to a fluctuating environment that fluctuates on a timescale longer than  $10^{-11}$  s [25]. The faster the environment fluctuations, the smaller the quadrupole splitting. Taking into account that both QS1 and QS2 quadrupole splittings decrease with increasing  $\text{Mn}^{4+}$  ion concentration and increase with decreasing temperature we suggest that two Fe positions in the  $\text{La}_{0.9}\text{Mn}_{0.975}\text{Fe}_{0.025}\text{O}_x$  lattice differ in the orbital dynamics of their manganese environment. We assume that the quadrupole

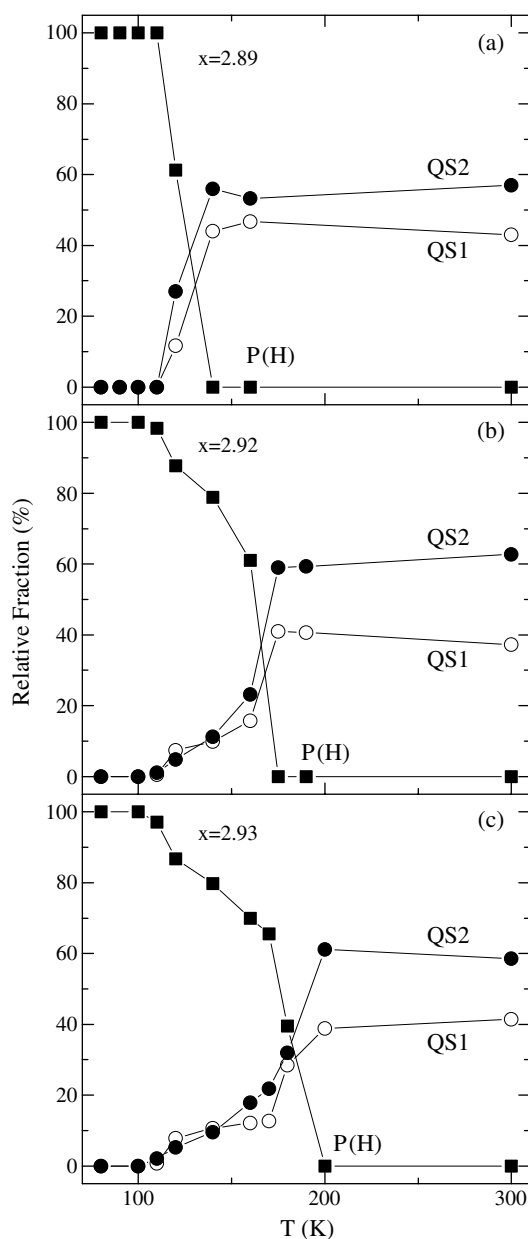


**Figure 6.** Relative fractions of the quadrupole doublets and Zeeman sextet as a function of temperature for  $x = 2.89, 2.92$  and  $2.93$  compounds.

doublet with the large quadrupole splitting QS1 corresponds to the Fe position, in which the non-Jahn–Teller  $\text{Fe}^{3+}$  ions are surrounded by six  $\text{Mn}^{3+}$  ions. At the high symmetry iron position with the smaller quadrupole splitting QS2, at least one of manganese ions surrounding the Fe position is in the  $\text{Mn}^{4+}$  state. Due to the unequal amount of non-Jahn–Teller ions in the  $\text{Fe}^{3+} + 6\text{Mn}^{3+}$  and  $\text{Fe}^{3+} + n\text{Mn}^{4+} + (6 - n)\text{Mn}^{3+}$  configurations, the orbital dynamics in these clusters have to be different. However, as a result of the 3D dynamic orbital correlations

described above, ferromagnetic ordering between the Mn ions is established in both these cases. The orbital dynamics becomes slower as the temperature decreases (table 2). It can be the driving force of the FMM to FMI phase transition observed for  $\text{La}_{1-x}\text{A}_x\text{MnO}_3$  ( $\text{A} = \text{Ca}, \text{Sr}; x \sim 0.15$ ) manganites with decreasing temperature [26], and the appearance of localized  $\text{Mn}^{3+,4+}$  states in metallic manganites at low temperatures, as evidenced by nuclear magnetic resonance measurements [8, 27]. The fact that the paramagnetic phase coexists with the magnetically ordered state in a wide temperature range, which increases with increasing  $\text{Mn}^{4+}$  content, suggests a non-statistical distribution of the  $\text{Mn}^{4+}$  and  $\text{Fe}^{3+}$  ions. The existence of consistent deviation from a random cation distribution in the solid solutions of  $\text{La}_{1-x}\text{Sr}_x\text{MnO}_3$  manganites is confirmed by x-ray absorption fine structure measurements [28]. The  $\text{Mn}^{4+}$ -rich clusters (which are probably located close to A-site vacancies due to the electroneutrality condition) with the faster orbital dynamics should have the higher temperature of the ferromagnetic ordering.

The studied  $\text{La}_{0.9}\text{Mn}_{0.975}\text{Fe}_{0.025}\text{O}_x$  samples are not purely ferromagnetic. The large difference between ZFC and FC curves observed for these samples below 110 K indicates the presence of an anisotropic magnetic coupling which differs from the isotropic ferromagnetic one [10]. The  $\text{Fe}^{3+}$ - and  $\text{Mn}^{4+}$ -free clusters seem to exhibit the static antiferrodistortive ordering of the  $d_{3z^2-r^2}$  orbitals which results in the antiferromagnetic order of the  $\text{Mn}^{3+}$  spins.

## 5. Conclusions

Mössbauer measurements of the  $\text{La}_{0.9}\text{Mn}_{0.975}\text{Fe}_{0.025}\text{O}_x$  ( $x = 2.89, 2.92$  and  $2.93$ ) samples were performed to reveal the coupling of magnetic properties of the manganites with the type of their orbital state. Iron in the  $\text{La}_{0.9}\text{Mn}_{0.975}\text{Fe}_{0.025}\text{O}_x$  lattice was found to be in the  $\text{Fe}^{3+}$  state with a high spin electronic configuration. At higher temperatures the Mössbauer spectra of all three samples are fitted with two quadrupole doublets which indicate two different iron positions. Some of the Fe ions occupy the low symmetry lattice position, as evidenced by the large value of quadrupole splitting QS1; the others are located in the more symmetric lattice position with the smaller quadrupole splitting QS2. Both QS1 and QS2 quadrupole splittings decrease with increasing  $\text{Mn}^{4+}$  ions concentration and increase with decreasing temperature. A slight increase of the relative fraction of Fe ions at the high symmetry lattice position with QS2 is observed with increasing  $\text{Mn}^{4+}$  content. In the magnetically ordered phase, the Mössbauer spectra are fitted with the hyperfine field distribution  $P(H)$  that consists of one dominating peak, suggesting one prevailing Fe site in the lattice, i.e. two high-temperature Fe positions become indistinguishable. It has been suggested that the two Fe positions in the  $\text{La}_{0.9}\text{Mn}_{0.975}\text{Fe}_{0.025}\text{O}_x$  lattice differ in the orbital dynamics of their manganese environment. In the position with the characteristic QS1 value, the  $\text{Fe}^{3+}$  is surrounded by six  $\text{Mn}^{3+}$  ions. The second iron position corresponds to the manganese environment in which at least one manganese ion is in the  $\text{Mn}^{4+}$  state. Due to removal of the static Jahn-Teller distortions, induced by the presence of non-Jahn-Teller  $\text{Fe}^{3+}$  and  $\text{Mn}^{4+}$  ions, the ferromagnetic ordering arises in the Mn environment of both Fe positions.

## Acknowledgments

This work was partly supported by the Belarus Fund for Basic Research (Project F03-120), GPOFI 'Nanomaterials and nanotechnologies' (Task Nanomaterials and nanotechnologies 3.3) and the State Committee for Scientific Research (Poland), grant number PBZ/KBN-013/T08.

## References

- [1] Wollan E O and Koehler W C 1955 *Phys. Rev.* **100** 545
- [2] Urushibara A, Moritomo Y, Arima T, Asamitsu A, Kido G and Tokura Y 1995 *Phys. Rev. B* **51** 14103
- [3] Schiffer P, Ramirez A P, Bao W and Cheong S-W 1995 *Phys. Rev. Lett.* **75** 3336
- [4] Zener C 1951 *Phys. Rev.* **82** 403
- [5] Dagotto E, Hotta T and Moreo A 2001 *Phys. Rep.* **344** 1
- [6] Millis A J, Littlewood P B and Shraiman B I 1995 *Phys. Rev. Lett.* **74** 5144
- [7] Papavassiliou G, Pissas M, Belesi M, Fardis M, Dolinsek J, Dimitropoulos C and Ansermet J P 2003 *Phys. Rev. Lett.* **91** 147205
- [8] Belesi M, Papavassiliou G, Fardis M, Pissas M, Wegrowe J E and Dimitropoulos C 2001 *Phys. Rev. B* **63** 180406
- [9] Endoh Y, Hirota K, Ishihara S, Okamoto S, Murakami Y, Nishizawa A, Fukuda T, Kimura H, Nojiri H, Kaneko K and Maekawa S 1999 *Phys. Rev. Lett.* **82** 4328
- [10] Troyanchuk I O, Khomchenko V A, Tovar M, Szymczak H and Bärner K 2004 *Phys. Rev. B* **69** 054432
- [11] Rodriguez-Carvajal J 1993 *Physica B* **192** 55
- [12] Brand R A, Lauer J and Herlach D M 1983 *J. Phys. F: Met. Phys.* **13** 675
- [13] Shannon R D 1976 *Acta Crystallogr. A* **32** 751
- [14] Ganguly R, Maignan A, Martin C, Hervieu M and Raveau B 2002 *J. Phys.: Condens. Matter* **14** 8595
- [15] Greenwood N N and Gibb T C 1971 *Mössbauer Spectroscopy* (London: Chapman and Hall)
- [16] Troyanchuk I O 1992 *Zh. Eksp. Teor. Fiz.* **102** 251
- [17] Goodenough J B 1963 *Magnetism and Chemical Bond* (New York: Interscience)
- [18] Rodriguez-Carvajal J, Hennion M, Moussa F, Moudou A H, Pinsard L and Revcolevschi A 1998 *Phys. Rev. B* **57** R3189
- [19] Sánchez M C, Subías G, García J and Blasco J 2003 *Phys. Rev. Lett.* **90** 045503
- [20] Louca D, Egami T, Brosha E L, Röder H and Bishop A R 1997 *Phys. Rev. B* **56** R8475
- [21] Mizokawa T, Khomskii D I and Sawatzky G A 2001 *Phys. Rev. B* **63** 024403
- [22] Goodenough J B, Wold A, Arnett R J and Menyuk N 1961 *Phys. Rev.* **124** 373
- [23] Troyanchuk I O, Bushinsky M V, Szymczak H, Bärner K and Maignan A 2002 *Eur. Phys. J. B* **28** 75
- [24] Goodenough J B, Dass R I and Zhou J 2002 *Solid State Sci.* **4** 297
- [25] Kolesnik S, Dabrowski B, Mais J, Brown D E, Feng R, Chmaissem O, Kruk R and Kimball C W 2003 *Phys. Rev. B* **67** 144402
- [26] Liu G-L, Zhou J-S and Goodenough J B 2001 *Phys. Rev. B* **64** 144414
- [27] Papavassiliou G, Fardis M, Belesi M, Maris T G, Kallias G, Pissas M, Niarchos D, Dimitropoulos C and Dolinsek J 2000 *Phys. Rev. Lett.* **84** 761
- [28] Shibata T, Bunker B, Mitchel J F and Schiffer P 2002 *Phys. Rev. Lett.* **88** 207205